Catalysis Letters, Vol. 116, Nos. 1–2, July 2007 (© 2007)
DOI: 10.1007/s10562-007-9114-9

Adsorption and reaction of CO on $CuO–CeO_2$ catalysts prepared by the combustion method

George Avgouropoulos and Theophilos Ioannides*

Foundation for Research and Technology-Hellas, Institute of Chemical Engineering and High Temperature Chemical Processes (FORTH/ICE-HT), Patras, GR-26504, Greece

Received 30 March 2007; accepted 30 March 2007

Temperature-programmed techniques were employed to investigate the interaction of CO with $CuO–CeO_2$ prepared by the urea-nitrates combustion method. These catalysts exhibited high and stable CO oxidation activity at relatively low reaction temperatures (< 150 °C). The CO adsorption capacity and catalytic activity of the catalysts was analogous to the concentration of easily-reduced copper oxide surface species. TPD and TPSR results can be explained by a dual scheme of CO adsorption: (i) on oxidized sites, which get reduced with simultaneous formation of surface CO_2 and (ii) on reduced sites created by the former interaction. 10–20% of adsorbed CO desorbs molecularly in the absence of gas-phase O_2, but reacts totally towards CO_2 in the presence of gas-phase O_2. Inhibition by CO_2 observed under steady-state CO oxidation conditions is due to CO_2 adsorption as found by CO_2-TPD.

KEY WORDS: CO oxidation; ceria; copper oxide; combustion method; TPD; TPSR.

1. Introduction

Copper-cerium oxide catalysts have been extensively examined as a possible substitute for precious metals, since they have much lower cost and comparable or even higher activity for CO oxidation. This reaction is of prime importance in air pollution control and purification of hydrogen-rich streams for fuel cell applications.

CeO_2 is one of the most thermally stable compounds and the oxidation state of the cerium cation may vary between $+3$ and $+4$ under various redox conditions. Ceria has distinct defect chemistry, ability to exchange lattice oxygen with the gas-phase and promotes CO removal through oxidation with lattice oxygen [1–7].

The beneficial catalytic properties of ceria are well represented in Cu–Ce oxide catalysts, which have been successfully tested in many catalytic reactions [3–13]. Liu and Flytzani-Stephanopoulos were the first to report that the Cu–Ce–O system is very active for complete oxidation of CO [3] with catalytic activity comparable or even superior to that of Pt-based catalysts. The redox properties of ceria can enhance the catalytic performance of copper oxide in CO oxidation reaction, since additional active sites, generated from oxygen vacancies, are present at the interface of the two phases [3, 7]. Concerning the nature of the active copper species, it is generally accepted that these are related to well-dispersed states of copper, probably in the form of copper oxide clusters in contact with the ceria and/or as an interfacial solid solution [3, 6–10, 13–23]. The correlation between the reducibility of highly dispersed copper oxide species and their catalytic activity appears to be well established [3, 5, 7, 8, 13, 16, 24–28]. A synergistic reaction model has been proposed in order to explain the enhanced catalytic activity shown by Cu–Ce oxide catalysts, in which Cu^{+} species stabilized by interactions between copper oxide clusters and cerium oxide provide surface sites for CO adsorption, while ceria provides the oxygen source [3]. The presence of both Cu^{2+} and Cu^{1+} species in the catalysts has been found by several investigators [3, 8, 9, 24]. Quantitative XPS analysis showed a significant enrichment of the surface with copper oxide species [8].

In this study, temperature-programmed techniques, such as TPD and TPSR of preadsorbed CO as well as TPD of preadsorbed CO_2, were used in order to examine the role of ceria on the adsorptive properties of combustion-synthesized $CuO–CeO_2$ catalysts. The effect of ceria on the adsorptive behavior of the $CuO–CeO_2$ catalysts was investigated and correlated with the catalytic performance in the CO oxidation reaction.

2. Experimental

2.1. Catalysts preparation

$CuO–CeO_2$ catalysts were prepared by the combustion method with cerium nitrate [$Ce(NO_3)_3 \cdot 6H_2O$], copper nitrate [$Cu(NO_3)_2 \cdot 3H_2O$] and urea [CH_4N_2O] as starting compounds [8]. The following catalysts were synthesized: CuO, CeO_2, $Cu_{0.10}Ce_{0.90}$, $Cu_{0.15}Ce_{0.85}$ and $Cu_{0.20}Ce_{0.80}$, where the index of Cu corresponds to the

*To whom correspondence should be addressed.
E-mail: theo@iceht.forth.gr

atomic ratio Cu/(Cu + Ce). An additional high-surface-area CuO sample, denoted as HS-CuO (S_{BET} = 21.3 m^2 g^{-1}) was prepared by a citrate method [4].

2.2. Catalyst characterization

Temperature Programmed Reduction (TPR), Temperature Programmed Desorption (TPD) and Surface Reaction (TPSR) experiments were carried out in a fixed-bed reactor system, described in detail elsewhere [8]. A mass spectrometer (Omnistar/Pfeiffer Vacuum) was used for on-line monitoring of effluent gases. Prior to each test, the catalyst (30–50 mg with particle size of $90 < d_p < 180$ μm) was treated under a 20% O_2/He mixture at 400 °C for 30 min, cooled under the same gas flow to 32 °C and purged with He. TPR experiments were performed under a flow of a 3% H_2/He mixture (50 cm^3 min^{-1}) using a heating rate of 20 °C min^{-1}. Adsorption of CO (CO-TPD and TPSR-O_2) or CO_2 (CO_2-TPD) was carried out under a flow of 1% CO/He or 1.5% CO_2/He mixture, respectively. Following completion of the adsorption, indicated by stable signals of CO or CO_2 in the mass spectrometer, the reactor was purged with pure He for ~10 min. Then, the TPD or TPSR run was started under a flow of 40 cm^3 min^{-1} He (CO-TPD and CO_2-TPD) or 1% O_2/He (TPSR-O_2) with a heating rate of 20 °C min^{-1}. In a preliminary study, the catalysts were characterized by BET, H_2-TPR, XRD and XPS [8]. The quantitative data of the deconvoluted components of experimental H_2-TPR profiles were determined with the use of PeakFit 4 and are presented in Table 1.

2.3. CO oxidation measurements

The catalytic oxidation of CO was carried out in a conventional flow system, previously described [8]. The feed gas was passed through a fixed bed reactor containing the catalyst (50–300 mg, 90–180 μm particle size). Prior to all catalytic tests, the samples were heated in a flowing 20 vol.% O_2/He mixture at 400 °C for 30 min, followed by cooling down to the reaction temperature in pure He. The total flow rate of the reaction mixture was 50–100 cm^3 min^{-1}, yielding contact times (W/F) in the range of 0.03–0.36 g s cm^{-3}. The feedstream contained 1 vol.% CO, 0.5 vol.% O_2, 0–1.5 vol.% CO_2, 0–1.5 vol.% H_2O, He balance. Product and reactant analysis was carried out by a gas chromatograph (Shimadzu GC-14B) equipped with a TCD.

3. Results and discussion

3.1. TPD of adsorbed CO or CO_2

The TPD profiles of CO and CO_2 after CO adsorption at RT over CuO–CeO_2 catalysts are shown in figure 1. The corresponding profiles of pure HS-CuO are also shown for comparison purposes. That oxide was synthesized under mild conditions in order to avoid extensive sintering of the material (which inherently takes place in the case of combustion-synthesized CuO) and thus be able to have measurable adsorbed quantities of CO or CO_2. The majority of adsorbed CO (~75–90%) is observed to desorb as CO_2, a fact that indicates reaction of adsorbed CO with surface oxygen [15, 5]. The CO_2 profiles are characterized by a main peak at ~108–118°C with a tail extending up to 350–400 °C.

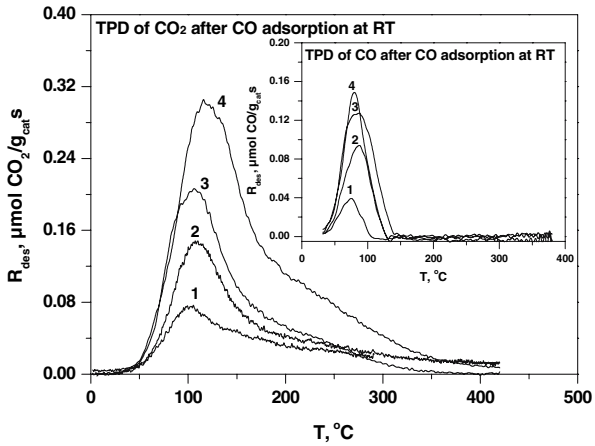

Figure 1. TPD profiles of CO_2 and CO (inset) after CO adsorption at RT, for pure HS-CuO (1) and for combustion-synthesized $Cu_{0.10}Ce_{0.90}$ (2), $Cu_{0.15}Ce_{0.85}$ (3) and $Cu_{0.20}Ce_{0.80}$ (4) catalysts.

Table 1
Characteristics of CuO–CeO_2 catalysts based on data presented in [8]

Catalyst	S_{BET} (m^2 g^{-1})	TPR peak maxima (T_i, °C) and contribution (H_2/Cu) of reducible species[a]				
		T_1	T_2	T_3	T_4	$(H_2)_{total}/(Cu)_{nominal}$
$Cu_{0.10}Ce_{0.90}$	25	163 (0.18)	217 (1.15)	256 (0.41)	290 (0.21)	1.95
$Cu_{0.15}Ce_{0.85}$	39	163 (0.25)	210 (0.89)	250 (0.40)	294 (0.21)	1.75
$Cu_{0.20}Ce_{0.80}$	24	161 (0.11)	211 (0.63)	255 (0.68)	300 (0.42)	1.84
CuO	3	–	–	–	295	0.99
CeO_2	10	–	–	–	–[b]	nm

[a]The values in parentheses represent the contribution of reducible species, expressed as a molar ratio of consumed H_2 per nominal loading of Cu (H_2/Cu), as determined by the deconvolution of TPR profiles in [8].
[b]No reduction peaks were observed at temperatures lower than 500 °C.

The CO_2 peak of $Cu_{15}Ce_{85}$ catalyst is slightly shifted to higher temperatures, probably due to re-adsorption phenomena, since the desorbed quantity of CO_2 is significantly higher in that case. A similar CO_2 profile was obtained for pure CuO, which consisted of a small peak at ~100 °C with a tail extending up to 300 °C. Regarding pure CeO_2, very small amounts of CO_2 were detected during TPD (not shown), with CO_2 appearing above 225 °C and slightly increasing with temperature. For all Cu-containing catalysts, small amounts of CO are desorbing at low temperatures with a single, symmetrical peak at 75–85 °C (inset of figure 1). CO desorption starts immediately upon initiation of the temperature ramp. The position and the shape of CO_2 and CO peaks suggest that the characteristics of CO adsorption over pure copper oxide remain the same upon addition of ceria. TPD profiles consisting of a small CO peak at 70–80 °C and a CO_2 peak at 110 °C with a tail extending up to 450 °C, have been also reported by Martinez-Arias et al. [15] for a 1% CuO/CeO_2 catalyst prepared by impregnation and activated at 500 °C. Luo et al. [5] reported negligible CO desorption during CO-TPD over CuO/CeO_2 catalysts (prepared by impregnation and calcined at various temperatures), while one CO_2 desorption peak was observed at about 110 °C. The adsorbed amount on pure CuO and CeO_2 was very small. Only one CO_2 desorption peak at about 110°C on CuO/CeO_2 was also observed by Lin et al. [29]. These results are quite similar to what was found in this work. Intact CO desorption (albeit at small amounts) during TPD implies that at least part of CO adsorbs molecularly and reversibly on the catalysts when the adsorption is carried out at RT. The main step of surface transformation of adsorbed CO with increase of temperature, however, appears to be its reaction with surface oxygen towards CO_2.

As TPD profiles of CO_2 include the desorption of significant amounts of CO_2 at high temperatures, i.e. at ~ 300–400 °C, this may be attributed either to decomposition of carbonates formed upon interaction of adsorbed CO with surface oxygen towards adsorbed CO_2, which is bound as carbonate species on the surface [5, 1, 15, 30–32] or to reaction of strongly bound CO with surface oxygen [33].

The quantities of desorbed CO_2 and CO (in μmol/g) following adsorption of CO at RT are presented in Table 2. It can be observed that: (i) the amount of CO desorbed is 10–25% of the total (CO + CO_2) amount desorbed from the catalysts, (ii) the amount of desorbed CO_2 is 2.5–4 times higher in CuO–CeO_2 catalysts compared to pure CuO and (iii) there appears no definite trend with copper content. Among the samples examined, the $Cu_{0.15}Ce_{0.85}$ adsorbed the highest amount of CO during CO adsorption, and most of that amount interacted with surface oxygen to a higher extent compared to the other samples. Recently, Jung et al. [34] reported that the total CO uptake of a 5 wt.% CuO–CeO_2 catalyst calcined at 700 °C is 240 μmol g^{-1}, of which ~50% (124 μmol g^{-1}) represents the irreversibly adsorbed CO (not desorbed under vacuum at 35 °C). Our results indicate a smaller CO uptake, which may be due to the much higher CO pressures (100–500 mmHg) employed by Jung et al.

TPD experiments of CO_2 desorption following adsorption of CO_2 at RT were also carried out in view of the inhibiting role of CO_2 in oxidation of CO over CuO–CeO_2 catalysts [8, 25]. The TPD profiles of CO_2 after its adsorption at RT are shown in figure 2 for CuO–CeO_2 catalysts as well as for pure HS-CuO and CeO_2. The shape of CO_2 peaks is quite similar with the CO_2 profiles after adsorption of CO at RT (figure 1). In the case of CuO-CeO_2 catalysts, a main CO_2 peak at ~88 °C was found with a tail up to 300–400 °C. However, the CO_2 peaks from CuO–CeO_2 appear at lower temperatures compared with the corresponding CO_2 peaks after CO adsorption (~ 108–118 °C). The shift is more intense for the $Cu_{15}Ce_{85}$ catalyst. The amounts of adsorbed CO_2 (per gram of catalyst) are considerably smaller than the amounts of adsorbed CO (Table 2), although the feed gas during adsorption contained 1.5% CO_2 compared to 1% CO in the case of CO-TPD. This implies that CO_2 adsorption is weaker than CO adsorption. For pure HS-CuO, CO_2 desorption took place in the form of a peak at 100 °C with a tail up to 300 °C. For pure CeO_2, the CO_2

Table 2
Desorbed amounts of CO or CO_2 after CO (CO-TPD and TPSR-O_2) or CO_2 (CO_2-TPD) adsorption at RT over CuO–CeO_2 catalysts

Catalyst	Desorbed amount of CO or CO_2, Q_{des}				
	CO-TPD			TPSR-O_2	CO_2-TPD
	μmol CO_2 g^{-1}	μmol CO g^{-1}	μmol (CO + CO_2) g^{-1}	μmol CO_2 g^{-1}	μmol CO_2 g^{-1}
$Cu_{0.10}Ce_{0.90}$	49.4	14.8	64.2	63.6	35.5
$Cu_{0.15}Ce_{0.85}$	111.5	19.7	131.2	130.5	43.4
$Cu_{0.20}Ce_{0.80}$	62.3	18.8	81.1	79.2	32.3
HS-CuO[a]	31.4	2.2	33.6	31.8	26.7
CeO_2	–	–	–	–	30.8

[a]High surface copper oxide prepared with the amorphous citrate method, hydrothermally treated at 150°C and calcined in air at 300°C. S_{BET} = 21.3 m^2 g^{-1}.

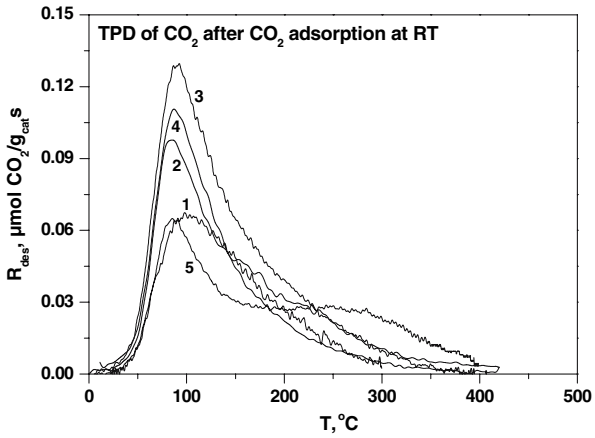

Figure 2. TPD profiles of CO_2 after CO_2 adsorption at RT, for pure HS-CuO (1) and for combustion-synthesized $Cu_{0.10}Ce_{0.90}$ (2), $Cu_{0.15}Ce_{0.85}$ (3), $Cu_{0.20}Ce_{0.80}$ (4) and CeO_2 (5) catalysts.

profile consisted of a low-temp main peak at 85 °C and a second -lower in intensity- peak at 250 °C. It has also to be noted that the amount of adsorbed CO_2 for CuO–CeO_2 catalysts seems to have quite similar values with those for pure CuO and pure CeO_2, implying that CO_2 adsorption on CuO–CeO_2 catalysts takes place on both CuO and CeO_2. In summary, CO_2-TPD has shown that:

- the adsorbed amounts of CO_2 are considerably smaller than those of CO
- the CO_2 peak from CO_2 adsorption appears at a lower temperature than the CO_2 peak from CO adsorption
- a similar tail in CO_2 peaks from both CO-TPD and CO_2-TPD is evident in the profiles.

Recently, Marino et al. [35] reported that under steady-state CO oxidation conditions in the presence of CO_2, the inhibition of CO_2 on catalyst activity diminishes with increase of reaction temperature allowing complete CO conversion to be achieved at temperatures around 160–200 °C. This is in accordance with the TPD results, which show that CO_2 desorption takes place at around 90 °C. It is expected, therefore, that the surface coverage of CO_2 will become quite low at temperatures around 130 °C or higher. In addition, one would expect stronger inhibition over pure CuO than on CuO–CeO_2 catalysts. This is due to: (i) the stronger adsorption of CO_2 on pure CuO compared to CuO–CeO_2 catalysts, as indicated by the higher CO_2 peak temperature in the former case and (ii) the higher value of the ratio CO_{ads}/CO_{2ads} on CuO–CeO_2 catalysts compared to pure CuO, indicating that CO_2 occupies a larger fraction of active sites on pure CuO, causing in this way a stronger inhibition.

3.2. TPSR of adsorbed CO with O_2

TPSR experiments following adsorption of CO at RT were carried out using an 1% O_2/He mixture as the carrier gas. No CO was found to desorb during the temperature ramp, in contrast to what was found during TPD experiments. Therefore, reversibly adsorbed CO gets oxidized in the presence of gas-phase oxygen. The only product detected in the gas-phase was CO_2. TPSR profiles of CO_2 from CuO–CeO_2 catalysts and pure HS-CuO are shown in figure 3. Compared to what happens in the absence of O_2 (figure 1), the reactivity of preadsorbed CO has significantly increased in the presence of gas-phase O_2 as deduced from the shift of CO_2 peaks to lower temperatures. All profiles are rather broad showing a tail extending up to 400 °C. On the other hand, the gas-phase oxygen does not appear to enhance the rate of oxidation of preadsorbed CO on pure HS-CuO and the CO_2 profiles during TPD and TPSR are quite similar. The amounts of CO_2 produced during TPSR from all catalysts examined are shown in Table 2. In all cases, the amounts of CO_2 produced during TPSR are almost equal to the sum of (CO + CO_2) produced during TPD of preadsorbed CO. This result, therefore, helps validate and confirm the corresponding TPD results.

In order to be able to compare more clearly the effect of gas-phase oxygen on the reactivity of adsorbed CO, the TPD and TPSR profiles of CO_2 from the $Cu_{0.15}Ce_{0.85}$ catalyst are shown in figure 4. It can be seen that heating in the presence of gas-phase oxygen enhances the rate of oxidation of preadsorbed CO. Taking into account that:

(i) the catalysts can be considered as fully oxidized before CO introduction because they were already pre-treated under an oxidative atmosphere,
(ii) if CO adsorption took place molecularly without any further reaction at RT, i.e. reaction with surface oxygen leading to adsorbed CO_2 or carbonate formation and to partial reduction of the surface (Cu^+ and/or Ce^{3+} ions), then one would not expect any

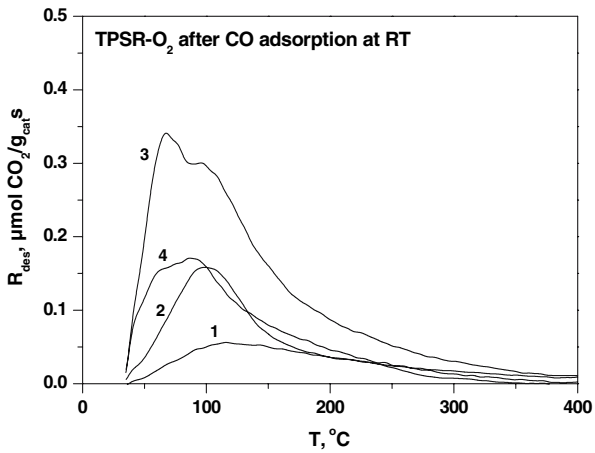

Figure 3. TPSR profiles of CO_2 (Carrier gas: 1% O_2/He), after adsorption of CO at RT, for pure HS-CuO (1) and for combustion-synthesized $Cu_{0.10}Ce_{0.90}$ (2), $Cu_{0.15}Ce_{0.85}$ (3) and $Cu_{0.20}Ce_{0.80}$ (4) catalysts.

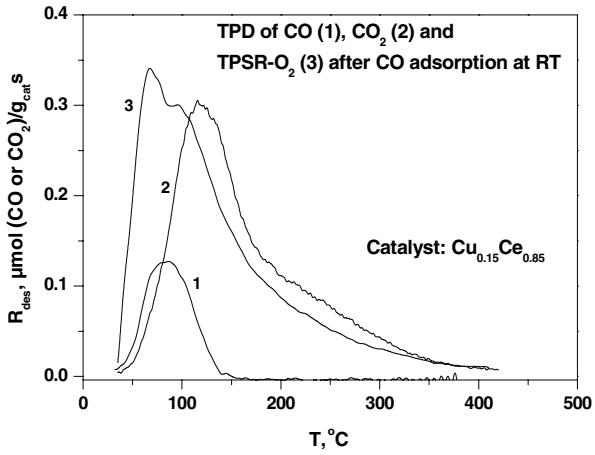

Figure 4. TPD profiles of CO (1) and CO_2 (2) along with TPSR profiles of CO_2 (Carrier gas: 1% O_2/He) after adsorption of CO at RT, for $Cu_{0.15}Ce_{0.85}$ catalyst.

important effect of the presence of gaseous O_2 upon initiation of the TPSR run, because the catalyst would already contain all the oxygen species it can accommodate.

Therefore, the TPSR results can only be explained assuming the occurrence of catalyst reduction upon introduction of CO at RT. It should be mentioned that no CO_2 was detected in the gas phase, during exposure of the catalysts to CO at RT implying that produced CO_2 remains on the surface because the temperature is low. Martinez-Arias et al. [36] have observed formation of Cu^+ carbonyls via FTIR spectroscopy by contacting a CuO–CeO_2 catalyst with CO at RT. They attribute this phenomenon to interaction of CO with Cu^{2+} ions with unsaturated coordination leading to their reduction with accompanying CO_2 formation. They did not observe CO_2 evolution in the gas-phase, but the large absorbance in the carbonate region of FTIR spectra indicated formation of carbonate species on the surface. Based on DRIFTS, FTIR and catalytic activity results, showing CO chemisorption at low temperatures, Martinez Arias et al. [15, 36] suggested the formation of carbonyl species upon CO adsorption on those reduced centers. An important question refers to which are the specific regions in the TPD and TPSR profiles of CO_2 corresponding to the decomposition of such carbonates. We propose that these regions are the ones, which are the least influenced by the presence of O_2 in the gas-phase, i.e. the long CO_2 tail from ~150–200 °C up to 400 °C. On the other hand, the similarity of TPD and TPSR profiles in the case of pure HS-CuO indicates either that reduction of the CuO surface does not take place upon exposure to CO at RT or that appearance of CO_2 in the gas-phase is limited by the process of desorption of CO_2.

Based on the TPD and TPSR results, we can postulate that upon exposure of the CuO–CeO_2 catalysts to CO at RT, CO adsorbs on the oxidized sites and reduces part of them itself being oxidized to adsorbed CO_2. CO can then adsorb on a reduced Cu^+ site. During TPD, CO adsorbed on Cu^+ desorbs molecularly but as temperature increases the possibility of further reaction with surface oxygen cannot be excluded. With further increase in temperature surface CO_2 desorbs from the catalyst. In the presence of gas phase O_2, the CO-Cu^+ species are highly reactive so that they appear as CO_2 in the TPSR profile (first low-temp peak). The second peak-during TPSR is essentially the CO_2 peak observed during TPD and is only slightly affected by the presence of O_2. Sedmak et al. [37] have carried out transient experiments in which they exposed the CuO–CeO_2 catalyst to isothermal step changes in CO concentration. They observed two peaks in the CO_2 response, which they attributed to: (i) adsorption of CO on an oxidized site and subsequent reduction of this site (first peak) and (ii) oxidation of CO adsorbed on a reduced Cu^+ site by catalyst oxygen (second peak). In our case, the peak sequence is reversed, because we add oxygen from the gas-phase which reacts with preadsorbed CO.

3.3. CO oxidation activity

Figure 5 shows the CO conversion as a function of temperature over the differently loaded CuO–CeO_2 catalysts. The corresponding curves of the pure oxides are not included in the same figure for reasons of clarity, since these samples exhibited poor activity towards CO_2 production. Thus, all the CuO-CeO_2 catalysts are significantly more active than the pure CuO and CeO_2 samples, indicative of an activity-enhancing synergy between the two phases. Among the catalysts prepared by the combustion method, the $Cu_{0.15}Ce_{0.85}$ catalyst showed the highest activity. Indeed, under our standard experimental conditions (W/F = 0.03 g s cm^{-3}, 1% CO, 0.5% O_2), the temperatures at which 50 and 99% conversion is obtained are significantly lower for the $Cu_{0.15}Ce_{0.85}$ catalyst as it can be seen in Table 3.

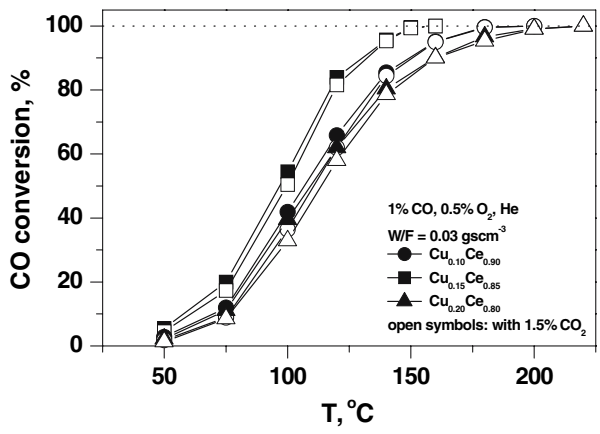

Figure 5. CO oxidation activity of $Cu_{0.10}Ce_{0.90}$ (●), $Cu_{0.15}Ce_{0.90}$ (■) and $Cu_{0.20}Ce_{0.90}$ (▲) catalysts at W/F = 0.03 g s cm^{-3}. The open symbols denote the presence of 1.5 vol.% CO_2 in the feed.

Table 3
Comparison of catalyst performance in CO oxidation[a]

Catalyst	r_{CO}, ($\mu mol_{CO}\ s^{-1}\ g^{-1}_{cat}$)			T_{50}[b], (°C)	T_{99}[b], (°C)
	50°C	75°C	100°C		
$Cu_{0.10}Ce_{0.90}$	0.41 (0.28)	1.75 (1.32)	6.22 (5.41)	106 (108)	177 (177)
$Cu_{0.15}Ce_{0.85}$	0.81 (0.65)	3.00 (2.60)	9.90 (9.70)	97 (99)	150 (150)
$Cu_{0.20}Ce_{0.80}$	0.33 (0.20)	1.65 (1.27)	5.87 (4.89)	110 (114)	200 (200)

[a]the values in parentheses were obtained in the presence of 1.5% CO_2 in the feed.
[b]W/F = 0.03 g s cm^{-3}.

Additionally, complete CO conversion can be achieved at 160 °C with the $Cu_{0.15}Ce_{0.85}$ catalyst, compared to 200 °C with the $Cu_{0.10}Ce_{0.90}$ catalyst and 220 °C with the $Cu_{0.20}Ce_{0.80}$ catalyst. The same trend of activity variation with copper loading is evident in the values of the CO oxidation rate, measured at three different temperatures, namely 50, 75 and 100 °C, and listed in Table 3. These values are 16–30 × and 160–300 × times higher than the corresponding values on pure CuO and ceria, respectively (not shown). Thus, the catalytic activity order for the composition range studied is the following: $CeO_2 << CuO << Cu_{0.20}Ce_{0.80} < Cu_{0.10}Ce_{0.90} < Cu_{0.15}Ce_{0.85}$. These results are in agreement with the catalytic activity order, previously reported, for the preferential CO oxidation reaction over these catalysts, where no hydrogen was oxidized at temperatures lower than 120–140 °C [8]. In a study over co-precipitated CuO–CeO_2 catalysts, similar values of the CO oxidation rate were determined, regardless of the presence of 50% H_2 in the feed [37]. Recently, we compared the CO oxidation activity of various CuO–CeO_2 catalysts reported in the literature, on the basis of calculated reaction rate at 75 °C. Despite the varying catalyst and operation parameters (preparation method, copper loading and partial pressures), the calculated reaction rates are all in the range of 1–3 $\mu mol\ g^{-1}\ s^{-1}$ [4], in agreement with the corresponding reaction rates measured in the present study.

The effect of the presence of 1.5% CO_2 in the reaction mixture on the activity of CuO–CeO_2 catalysts is also shown in figure 5. The investigation of the role of CO_2 is interesting from the fact that CO_2 acts as an inhibitor of the CO oxidation reaction [8, 23, 25, 33, 35, 38]. However, the presence of 1.5% CO_2 in the feed induced a minimal loss in the catalytic activity, which disappeared at temperatures higher than 100–120 °C. Taking into account previous studies over the same catalytic system [8, 23, 25, 33, 35, 38], which reported a significant shift of the activity curves to higher temperatures, by about 20–40 °C, in the presence of 15% CO_2 in the feed, it is evident that the inhibiting effect is more pronounced as the CO_2 concentration in the feed increases [35]. Anyway, TPD following exposure of catalysts to CO_2 showed that CO_2 also adsorbs on the catalysts surface, thus explaining the inhibition of CO_2 observed under steady-state CO oxidation conditions. CO_2 desorption takes place at around 90 °C. When the CO oxidation reaction temperature is lower than the desorption temperature of CO_2, the catalytic activity will be diminished due to the adsorption of CO_2 on the active sites [33]. It is expected, therefore, that the surface coverage of CO_2 will become quite low at temperatures higher than 130 °C, and the inhibition will be eliminated. Regardless of the presence of CO_2, the same trend of the activity with the copper loading of the catalysts is observed. However, the inhibiting effect of CO_2 was more intense in the case of pure copper oxide, since the ratio of the reaction rate in the presence of CO_2 to the reaction rate in the absence of CO_2 at temperatures lower than 100 °C was significantly lower than 1. Therefore, addition of CeO_2 makes the catalysts more tolerant towards deactivation by CO_2.

The effect of contact time on the catalytic activity of $Cu_{0.15}Ce_{0.85}$ sample is shown in figure 6. With an increase in the contact time the activity curve is shifted to lower temperatures. Indeed, complete CO conversion can be achieved at ~110 °C with a W/F ratio equal to 0.36 g s cm^{-3}, compared to 160 °C with W/F = 0.03 g s cm^{-3}. In agreement with the above discussion, the inhibiting effect of the presence of 1.5% CO_2 in the feed,

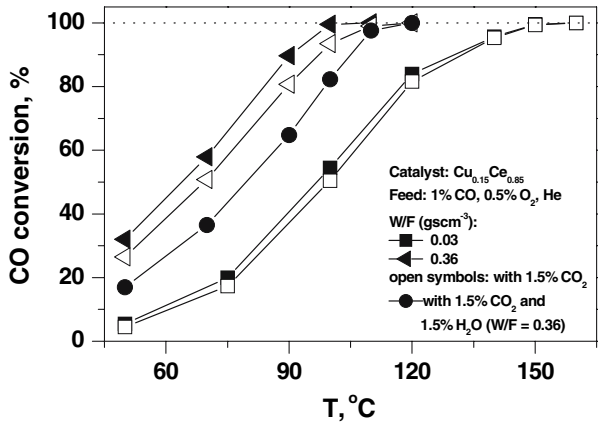

Figure 6. CO oxidation activity of $Cu_{0.15}Ce_{0.85}$ catalyst at W/F = 0.03 (■) and 0.36 (◀) g s cm^{-3}. The open symbols denote the presence of 1.5 vol.% CO_2 in the feed, while the circle symbols denote the presence of both 1.5 vol.% CO_2 and 1.5 vol.% H_2O in the feed (W/F = 0.36 g s cm^{-3}).

on the catalytic activity, is evident only at temperatures lower than 100 °C (figure 6). In addition with the CO_2 effect, the influence of the presence of 1.5% H_2O in the CO_2-containing feed was examined for the $Cu_{0.15}Ce_{0.85}$ sample (figure 6). At temperatures up to 100 °C, the catalyst lost a significant portion of its initial activity when both CO_2 and H_2O are present in the feed and a given CO conversion can be obtained at a temperature higher by about 20 °C. Complete CO conversion was achieved at ~110 °C, regardless of the presence of CO_2 and H_2O in the feedstream. The presence of water vapor induced a more significant loss on the catalyst activity only at temperatures lower than 100 °C, probably due to desorption of water above that temperature [33]. The $Cu_{0.15}Ce_{0.85}$ catalyst was also tested for its performance with reaction time at two different temperatures, namely at 90 and 110 °C. As shown in figure 7, the catalyst exhibited a stable behavior in both reaction temperatures, regardless of the presence of CO_2 and H_2O in the feed. In agreement with the above discussion, the presence of H_2O provoked a higher degree of deactivation but only at the lower temperature. However, preliminary studies showed that this inhibition by the presence of CO_2 and H_2O is not irreversible and the only consequence at temperatures lower than 110 °C, is that higher contact or higher reaction temperature is required in order to achieve the same CO conversion.

3.4. Promoting role of CeO_2

The promoting role of CeO_2 is evident, first of all, in the structural characteristics of CuO–CeO_2 catalysts, i.e. in the enhancement of their specific surface area which becomes optimal for the composition $Cu_{0.15}Ce_{0.85}$ (Table 1). A similar behavior is found for CuO–CeO_2 catalysts prepared by a modified citrate method [4]. The optimal $Cu_{0.15}Ce_{0.85}$ catalyst has also the highest amount of easily reduced species (Table 1). The hydrogen consumption values during TPR up to the temperature of 500 °C (Table 1) are significantly higher than the theoretical ones corresponding to the complete reduction of Cu^{2+} to Cu^0. The H_2/Cu molar ratio was found to be 1.75–1.95 for the combustion-synthesized catalysts and there is no definite trend with copper content. These values are slightly higher than the reported values of 1.65 over $Ce_{0.95}Cu_{0.05}O_y$ by Shan et al. [22] and 1.3 over 10–15 at.% Cu/CeO_2 catalysts by Gayen et al. [28]. Much higher values were reported for low copper loadings (< 5 at.%) [28].

There exists a direct analogy between the amount of easily reduced species and the quantity of adsorbed CO. The quantities of adsorbed CO (Table 2) are 56–59% of the corresponding hydrogen consumption values of the first deconvoluted peak. It is, therefore, quite plausible to assume that CO adsorption takes place mainly on these easily-reducible sites. These sites have a higher surface density on CuO–CeO_2 than on CuO, as can be deduced by comparing the amounts of adsorbed CO per unit surface area of the catalysts (these are 2.57–3.38 μmol m^{-2} for CuO-CeO_2 and 1.6 μmol m^{-2} for pure CuO). Based on the above, we can postulate that well-dispersed copper oxide species having a wide interface perimeter with ceria constitute the preferred adsorption sites for CO [5] and, as a consequence, the active sites for the reaction. The enhanced reducibility could be related to the higher oxygen mobility of the defective ceria structure created upon substitution of Ce^{4+} ions by Cu^{2+} or Cu^{1+} ions at the interface of both oxides [6, 7, 9, 20, 21, 27]. TPSR results have shown that CO can reduce Cu^{2+} even at room temperature, while CO adsorbed on reduced sites is highly reactive with gas-phase oxygen. On the other hand, pure CuO or ceria didn't show any similar redox behavior, thus indicating that the above properties resulted by strong interaction of both oxides.

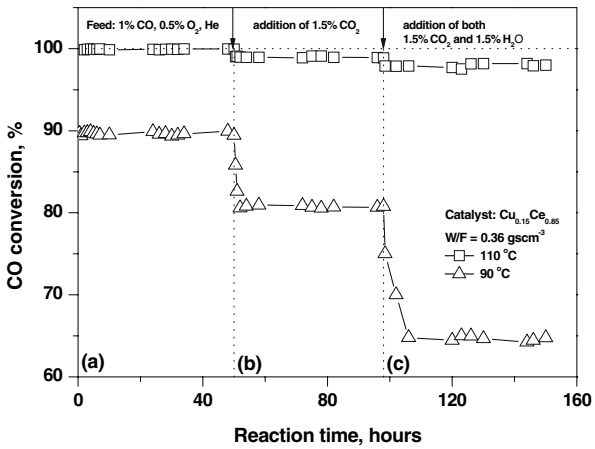

Figure 7. Variation of CO conversion with the reaction time at 90 (Δ) and 110 °C (□) and at W/F = 0.36 g s cm^{-3} over the $Cu_{0.15}Ce_{0.85}$ catalyst, in the absence of CO_2 and H_2O (a), in the presence of 1.5 vol.% CO_2 (b), and in the presence of both 1.5 vol.% CO_2 and 1.5 vol.% H_2O (c) in the feed.

4. Conclusions

The optimal CO oxidation CuO–CeO_2 catalyst when synthesized by the combustion method with urea as fuel has an atomic ratio of Cu/(Cu + Ce) = 0.15 and is characterized by the following properties:

- A reproducibly-obtained, larger specific surface area than all other compositions
- The highest concentration of easily reduced sites
- The highest CO adsorption capacity.

We found a direct correlation between the amount of easily reduced sites and the one of adsorbed CO. Adsorption of CO proceeds through initial reduction of Cu^{2+} and formation of adsorbed CO_2 followed by adsorption of CO on reduced Cu^{+} centres. The inhibition of CO oxidation by the presence of CO_2 is elimi-

nated at temperatures higher than the desorption temperature of CO_2 as found by TPD. The promoting role of ceria can be attributed to the creation of additional sites for CO adsorption and reaction, which get easily reduced.

References

[1] A. Trovarelli, Catal. Rev.-Sci. Eng. 38 (1996) 439.
[2] J. Kaspar, P. Fornasiero and M. Graziani, Catal. Today 50 (1999) 285.
[3] W. Liu and M.F. Stephanopoulos, J. Catal. 153 (1995) 304.
[4] G. Avgouropoulos and T. Ioannides, Appl. Catal. B: Environ. 67 (2006) 1.
[5] M. Luo, Y. Zhong, X. Yuan and X. Zheng, Appl. Catal. A: Gen. 162 (1997) 121.
[6] J. Xiaoyuan, L. Guanglie, Z. Renxian, M. Jianxin, C. Yu and Z. Xiaoming, Appl. Surf. Sci. 173 (2001) 208.
[7] J. Wang, D. Tsai and T. Huang, J. Catal. 208 (2002) 370.
[8] G. Avgouropoulos and T. Ioannides, Appl. Catal. A: Gen. 244 (2003) 155.
[9] S. Hocevar, U.O. Krasovec, B. Orel, A.S. Arico and H. Kim, Appl. Catal. B: Environ. 28 (2000) 113.
[10] P. Bera, S.T. Aruna, K.C. Patil and M.S. Hegde, J. Catal. 186 (1999) 36.
[11] Y. Li, Q. Fu and M. Flytzani-Stephanopoulos, Appl. Catal. B: Environ. 27 (2000) 179.
[12] J. Papavasiliou, G. Avgouropoulos and T. Ioannides, Catal. Commun. 5 (2004) 231.
[13] X. Tang, B. Zhang, Y. Li, Y. Xu, Q. Xin and W. Shen, Appl. Catal. A: Gen. 288 (2005) 116.
[14] P.G. Harrison, I.K. Ball, W. Azelee, W. Daniell and D. Goldfarb, Chem. Mater. 12 (2000) 3715.
[15] A. Martinez-Arias, M. Fernandez-Garcia, O. Galvez, J.M. Coronado, J.A. Anderson, J.C. Conesa, J. Soria and G. Munuera, J. Catal. 195 (2000) 207.
[16] X. Tang, B. Zhang, Y. Li, Y. Xu, Q. Xin and W. Shen, Catal. Today 93–95 (2004) 191.
[17] G. Marban and A.B. Fuertes, Appl. Catal. B: Environ. 57 (2004) 43.
[18] A. Martinez-Arias, A.B. Hungria, M. Fernandez-Garcia, J.C. Conesa and G. Munuera, J. Power Sources 151 (2005) 32.
[19] A. Pintar, J. Batista and S. Hocevar, J. Colloid Interf. Sci. 285 (2005) 218.
[20] C. Lamonier, A. Ponchel, A. D'Huysser and L. Jalowiecki-Duhamel, Catal. Today 50 (1999) 247.
[21] P. Bera, K.R. Priolkar, P.R. Sarode, M.S. Hegde, S. Emura, R. Kumashiro and N.P. Lalla, Chem. Mater. 14 (2002) 3591.
[22] W. Shan, W. Shen and C. Li, Chem. Mater. 15 (2003) 4761.
[23] C.M. Bae, J.B. Ko and D.H. Kim, Catal. Commun. 6 (2005) 507.
[24] A. Tschope, M. Trudeau and J. Ying, J. Phys. Chem. B 103 (1999) 8858.
[25] G. Avgouropoulos, T. Ioannides and H. Matralis, Appl. Catal. B: Environ. 56 (2005) 87.
[26] S. Zhang, W. Huang, X. Qiu, B. Li, X. Zheng and S. Wu, Catal. Lett. 80 (2002) 41.
[27] J.B. Wang, S. Lin and T. Huang, Appl. Catal. A: Gen. 232 (2002) 107.
[28] A. Gayen, T. Baidya, A.S. Prakash, N. Ravishankar and M.S. Hegde, Ind. J. Chem. A 44 (2005) 34.
[29] R. Lin, M. Luo, Y. Zhong, Z. Yan, G. Liu and W. Liu, Appl. Catal. A: Gen. 255 (2003) 331.
[30] F. Bozon-Verduraz and A. Bensalem, J. Chem. Soc. Faraday Trans. 90 (1994) 653.
[31] C. Li, Y. Sakata, T. Arai, K. Domen, K. Maruya and T. Onishi, J. Chem. Soc. Faraday Trans. 85 (1989) 929.
[32] S. Hilaire, X. Wang, T. Luo, R.J. Gorte and J. Wagner, Appl. Catal. A 215 (2001) 271.
[33] J. Park, J. Jeong, W. Yoon, C.S. Kim, H. Jung, H. Lee, D. Lee, Y. Park and Y. Rhee, Appl. Catal. A: Gen 274 (2004) 25.
[34] C.R. Jung, J. Han, S.W. Nam, T. Lim, S. Hong and H. Lee, Catal. Today 93–95 (2004) 183.
[35] F. Marino, C. Descorme and D. Duprez, Appl. Catal. B: Environ. 58 (2005) 175.
[36] A. Martinez-Arias, M. Fernandez-Garcia, J. Soria and J.C. Conesa, J. Catal. 182 (1999) 367.
[37] G. Sedmak, S. Hocevar and J. Levec, J. Catal. 222 (2004) 87–99.
[38] G. Avgouropoulos, T. Ioannides, H. Matralis, J. Batista and S. Hocevar, Catal. Lett. 73 (2001) 33.